Numerical Simulation of Controlled Nifedipine Release from Chitosan Microgels

Hua Li, Guoping Yan, Shunnian Wu, Zijie Wang, K. Y. Lam

Institute of High Performance Computing, National University of Singapore, 1 Science Park Road, #01-01, The Capricorn, Singapore Science Park II, Singapore 117528

Received 4 September 2003; accepted 3 March 2004
DOI 10.1002/app.20652
Published online in Wiley InterScience (www.interscience.wiley.com).

ABSTRACT: The numerical simulating investigation of drug delivery can provide deeper insight into drug release mechanisms and elucidate efficiently the influences of various physical parameters. Controlled nifedipine release from nonswellable chitosan sphere-based microgels is investigated numerically with a mathematical model in this article. The mathematical model takes into account both drug dissolution and drug diffusion through the continuous matrices of the spherical microgels. Meshless Hermite-cloud method is employed to solve the formulated partial differential equations. It is seen that the model well describes the nifedipine release process from the spherical chitosan microgels. The effect of several important physical parameters on drug release is evaluated, which include microsphere radius, equivalent drug saturation concentration, drug diffusion coefficient, and drug dissolution rate constant. © 2004 Wiley Periodicals, Inc. J Appl Polym Sci 93: 1928–1937, 2004

Key words: modeling; simulation; drug delivery systems; kinetics; microgels

INTRODUCTION

Nifedipine is a poorly water-soluble drug with solubility less than 10 mg/L.[1] As a well-known calcium channel blocker, nifedipine is most commonly used for the treatment of hypertension, a chronic disease that affects 10–20% of the world population and induces cardiovascular complications.[2] However, many serious adverse effects associated with immediate nifedipine release have been revealed, such as hypotension, myocardial ischemia or infarction, ventricular fibrillation, and cerebral ischemia.[3] Given the seriousness of the reported adverse events and the lack of any clinical documentation attesting to a benefit, the Food and Drug Administration (FDA) of the USA concluded that the use of immediately released nifedipine for hypertensive emergencies is neither safe nor effective, and therefore, should not be used.[4]

Microspheric drug release system has increasingly attracted attention recently.[5] Controlled nifedipine release was investigated by using various polymer-based microgels, such as spherical chitosan microgels,[6–7] Eudragit microcapsules,[2,8] and poly(D,L-lactide-*co*-glycolide acid) microspheres.[9–10] Obviously, the microspheric nifedipine release system reduces the total administration frequency to the patient. It is probably cycled over a long period, or triggered by specific environment or external events. Microspheric nifedipine release can maintain nifedipine at desired levels over a long period and thus eliminate the potential for both under- and overdosing. Consequently, it decreases the possible adverse effects of immediate nifedipine release. Additional advantages of microspherical nifedipine release include optimal administration dosage, better patient compliance, and improved drug efficacy.

The underlying drug release mechanisms for polymer-based microgels have obtained much understanding. When drug-loaded polymeric microgels are placed in contact with release medium, the drug release process can be divided into these four consecutive steps[2]: the imbibition of release medium into the microspherical system driven by osmotic pressure arising from concentration gradients, drug dissolution, drug diffusion through the continuous matrices of microgels due to concentration gradients, and drug diffusional and convective transport within the release medium. One or more of these steps can control the drug release process. Varshosaz and Falamarzian claimed that the drug release process could be via the diffusion through the continuous matrices or drug dissolution mechanism.[11] In the diffusion mechanism, drug diffusion through the continuous matrices of microgels controls the drug release process, whereas, in the dissolution mechanism, the drug release is controlled by the process involving drug dissolution within the microgels followed by drug diffusion through the continuous matrices of microgels. However, the drug release process is usually modeled with

Correspondence to: H. Li (lihua@ihpc.a-star.edu.sg).

the classical Fick's diffusion equation integrating with appropriate boundary conditions or with the simplified expressions developed by Higuchi and Higuchi.[12–15] A mathematical theory with simultaneous consideration of drug dissolution and diffusion in the continuous matrices of microgels was put forward by Grassi et al.[16] and fitted well to the experimentally measured temazeoan and medroxyprogesterone acetate release data. Recently, Hombreiro-Perez et al.[2] pointed out that an adequate description of nifedipine release from microgels must consider drug dissolution, drug diffusion in the continuous matrices of microgels, and the limited solubility of nifedipine in the release medium. Unfortunately, no effort was made to model the nifedipine release process because of the complexity.

The objective of this work was to investigate the nifedipine (Pliva, Croatia) release from chitosan microgels (Protan Laboratories, Inc., Drammen, Norway) by a mathematical model incorporating this complexity. The drug diffusion coefficient and drug dissolution rate constants were identified numerically by using the model. The effect of several physical parameters on drug release is simulated and discussed in detail, which include microsphere radius, drug saturation concentration, drug diffusion coefficient, and drug dissolution rate constant.

MATHEMATICAL MODEL AND IMPLEMENTATION

Model development

The initial drug loading concentration C_0 in spherical microgels is generally greater than the drug saturation concentration C_s. This can be achieved either by preparation of a solution and total evaporation of the solvent or by partial evaporation or phase inversion.[12] When the polymeric microgels are put into a well-stirred release medium, the following four mass transfer steps take place consequently[2]: (1) drug dissolution within the microgels; (2) drug diffusion within the matrices of microgels; (3) drug diffusion through the unstirred liquid boundary layers on the surfaces of the microgels; and (4) drug diffusion and convection within the release medium. Because the convective transport within the medium is usually fast compared with that of the diffusive mass, the convective transport can be neglected when calculating the overall rate of drug release from the polymeric microgels.[2] Therefore, it is reasonable to assume that drug dissolution and diffusion from the continuous matrices of spherical nonswellable microgels control the drug release in a well-stirred release medium.

The kinetics of drug release from the microgels with radius R can be simulated mathematically by the following partial differential governing equation[2]

$$\frac{\partial C(r,t)}{\partial t} = D\left(\frac{\partial^2 C(r,t)}{\partial r^2} + \frac{2}{r}\frac{\partial C(r,t)}{\partial r}\right) + k[\varepsilon C_s - C(r,t)] \quad (1)$$

and the initial and boundary conditions below for the drug release process in a well-stirred release medium,

$$t = 0 \quad 0 < r < R \quad C(r,t) = \varepsilon C_s \quad (2a)$$

$$t > 0 \quad r = 0 \quad \frac{\partial C(r,t)}{\partial r} = 0 \quad (2b)$$

$$t > 0 \quad r = R \quad C(r,t) = 0 \quad (2c)$$

where $C(r, t)$ (g/cm^3) is the drug concentration in the radial position r (cm) of the microgel system at the release time t (s). D (cm^2/s) is the drug diffusion coefficient, k (s^{-1}) is the first-order drug dissolution rate constant, ϵ is a parameter for the polymeric network meshes of microgels and is directly related to the crosslinking density of the polymeric microspheres. If C_s (g/cm^3) is defined as drug saturation concentration in the system, ϵC_s (g/cm^3) refers to the equivalent drug saturation concentration in microgels with a network mesh parameter ϵ.

The first term of the right-hand side in eq. (1) is the well-known Fick's second law of diffusion for a spherical system,[17] which describes the diffusional drug release process in the microgels due to the continuous dissolution of the drug. The second term on the right-hand side in eq. (1) corresponds to the potential rate-limiting drug dissolution process.[12] It is observed that, when the drug loading concentration C_0 is smaller than the drug saturation concentration C_s, eq. (1) is reduced to the classic Fick's diffusion equation. Although the drug diffusion coefficient D in the polymeric microgels may be solvent-concentration-dependent, usually it is reasonable to assume approximately a constant D for simplicity.

It is assumed that the drug is uniformly distributed throughout the microgels with equivalent drug saturation concentration ϵC_s initially. Under perfect sink conditions, the release medium can be considered to be well stirred; thus, the drug concentration outside of microgels is further assumed to be constant and equal to zero.

By defining dimensionless parameters,[12] $\xi = r/R$ for dimensionless radius, $\tau = Dt/R^2$ for dimensionless Fourier time, $\beta = kR^2/D$ called dimensionless dissolution/diffusion number, and dimensionless concentration $\psi(\xi, \tau) = 1 - C(r, t)/\epsilon C_s$, which indicates the nondimensional drug concentration additionally required to reach saturation dissolution, the partial differential governing equation, and initial and boundary conditions are thus rewritten in the dimensionless forms as,

$$\frac{\partial \psi(\xi,\tau)}{\partial \tau} = \frac{\partial^2 \psi(\xi,\tau)}{\partial \xi^2} + \frac{2}{\xi}\frac{\partial \psi(\xi,\tau)}{\partial \xi} - \beta\psi(\xi,\tau) \quad (3)$$

$$\tau = 0 \quad 0 < \xi < 1 \quad \psi(\xi, \tau) = 0 \tag{4}$$

$$\tau > 0 \quad \frac{\partial \psi(\xi, \tau)}{\partial \xi} = 0 \quad \text{at } \xi = 0, \quad \text{and} \quad \psi(\xi, \tau) = 1 \quad \text{at } \xi = 1 \tag{5}$$

After solving the set of above governing equations and conditions, $\psi(\xi, \tau)$ is obtained and then the drug concentration $C(r, t)$ is computed. According to Fick's first law,[18] the flux $J = J(r, t)$, the rate of drug transfer per unit area of section, is considered as

$$J(r, t) = -D \frac{\partial C(r, t)}{\partial r} \tag{6}$$

The rate of drug release from the microgels is thus calculated by[18]

$$\frac{\partial M_t}{\partial t} = AJ(r, t)|_{r=R} \tag{7}$$

where A is the area of microgels with radius R, M_t represents the amount of drug released after time t and can be calculated by integrating eq. (7)

$$M_t = \int_0^t AJ(r, \bar{t})|_{r=R} d\bar{t} = 4\pi R^2 \int_0^t \left(-D \frac{\partial C(r, \bar{t})}{\partial r}\bigg|_{r=R} \right) d\bar{t} = -4\pi R^2 D \int_0^t \frac{\partial C(r, \bar{t})}{\partial r}\bigg|_{r=R} d\bar{t} \tag{8}$$

Meshless Hermite-cloud method

The numerical technique employed in this work is the true meshless Hermite-cloud method, which is based on the Hermite interpolation theorem and the fixed kernel approximation.[19] Compared with the finite element method as traditionally principal numerical analysis tool for the modeling and simulation of wide-range science and engineering problems, the present meshless Hermite-cloud method is highly efficient because it does not require the construction of meshes or elements with high computational cost. Moreover, compared with generic weak-form meshless techniques, the present Hermite-cloud method, as a collocation-based true meshless strong-form procedure, is a much simpler implementation because no weak-form integration is required.

By using the Hermite-cloud method, an approximation $\tilde{f}(x)$ of a one-dimensional unknown real function $f(x)$ can be constructed by

$$\tilde{f}(x) = \sum_{n=1}^{N_T} N_n(x) f_n + \sum_{m=1}^{N_S} \left(x - \sum_{n=1}^{N_T} N_n(x) x_n \right) M_m(x) g_{xm} \tag{9}$$

where N_T and N_S ($\leq N_T$) are the total numbers of scattered points, covering both the interior computational domain and the surrounding edges, for the point values f_n and g_{xm}, respectively. f_n is the point value of unknown real function $f(x)$ at the nth point, and g_{xm} is the point value of the first-order differential, $g_x(x) = df(x)/dx$, at the mth point. The corresponding discrete approximation is written as

$$\tilde{g}_x(x) = \sum_{m=1}^{N_S} M_m(x) g_{xm} \tag{10}$$

In eq. (9), the shape function $N_n(x)$ and $M_m(x)$ for the functions $f(x)$ and $g_x(x)$, respectively, are defined as[20]

$$N_n(x) = \mathbf{B}(u_n)\mathbf{A}^{-1}(x_k)\mathbf{B}^T(x)K(x_k - u_n)\Delta L_n \quad n = 1, 2, \ldots, N_T \tag{11}$$

$$M_m(x) = \tilde{\mathbf{B}}(u_m)\tilde{\mathbf{A}}^{-1}(x_k)\tilde{\mathbf{B}}^T(x)K(x_k - u_m)\Delta L_m \quad m = 1, 2, \ldots, N_S \tag{12}$$

in which ΔL_n is defined as the cloud length of the nth point, $\mathbf{B}(u)$ and $\tilde{\mathbf{B}}(u)$ are the linearly independent basis-function vectors which are given by

$$\mathbf{B}(u) = \{b_1(u), b_2(u), b_3(u)\} = \{1, u, u^2\} \tag{13}$$

$$\tilde{\mathbf{B}}(u) = \{b_1(u), b_2(u)\} = \{1, u\} \tag{14}$$

and $\mathbf{A}(x_k)$ and $\tilde{\mathbf{A}}(x_k)$ are symmetric constant matrices corresponding to the central point x_k of the fixed cloud

$$A_{ij}(x_k) = \sum_{n=1}^{N_T} b_i(u_n)K(x_k - u_n)b_j(u_n)\Delta L_n \quad (i, j = 1, 2, 3) \tag{15}$$

$$\tilde{A}_{ij}(x_k) = \sum_{m=1}^{N_S} b_i(u_m)K(x_k - u_m)b_j(u_m)\Delta L_m \quad (i, j = 1, 2) \tag{16}$$

where $K(x_k - u)$ is a kernel function constructed by cubic spline function as

$$K(x_k - u) = \frac{1}{\Delta L_k}\begin{cases} 0 & 2 < z \\ (2-z)^3/6 & 1 \le z \le 2 \\ (2/3) - z^2(1 - z/2) & 0 \le z \le 1 \end{cases} \tag{17}$$

where $z = |(x_k - u)|/\Delta L_k$.

Because the additional unknown function $g_x(x)$ is introduced, the auxiliary condition is required to implement the Hermite-cloud method. Imposing the first-order partial differential with respect to x on the approximation $\tilde{f}(x)$ expressed by eq. (9), and noting eq. (10), the auxiliary condition is obtained as

$$\sum_{n=1}^{N_T} N_{n,x}(x) f_n - \sum_{m=1}^{N_S}\left(\sum_{n=1}^{N_T} N_{n,x}(x) x_n\right) M_m(x) g_{xm} = 0 \tag{18}$$

where $N_{n,x}(x)$ denotes the first derivative of $N_n(x)$ with respect to the variable x.

The formulation of the present Hermite-cloud method has thus far been completed and is able to solve generic engineering partial differential boundary value (PDBV) problems, such as

$$Lf(x) = P(x) \quad \text{PDEs in computational domain } \Omega \tag{19}$$

$$f(x) = Q(x) \quad \text{Dirichlet boundary condition on } \Gamma_D \tag{20}$$

$$\partial f(x)/\partial n = R(x) \quad \text{Neumann boundary condition on } \Gamma_N \tag{21}$$

where L is differential operator and $f(x)$ is an unknown real function. By using the point collocation technique, the approximation of the above PDBV problem can be expressed in discrete forms as

$$L\tilde{f}(x_j) = P(x_j) \quad (j = 1, 2, \ldots, N_\Omega) \tag{22}$$

$$\tilde{f}(x_j) = Q(x_j) \quad (j = 1, 2, \ldots, N_D) \tag{23}$$

$$\partial\tilde{f}(x_j)/\partial n = R(x_j) \quad (j = 1, 2, \ldots, N_N) \tag{24}$$

where N_Ω, N_D, and N_N are the numbers of scattered points in the interior computational domain and along the Dirichlet and Neumann edges, respectively. Thus, total number of scattered points $N_T = N_\Omega + N_D + N_N$.

Substituting eqs. (9) and (10) into eqs. (22)–(24) and considering the auxiliary condition (18), a set of discrete algebraic equations with respect to unknown point values f_i and g_{xi} is derived in matrix form as

$$[H_{ij}]_{(N_T+N_S)\times(N_T+N_S)}\{F_i\}_{(N_T+N_S)\times 1} = \{d_i\}_{(N_T+N_S)\times 1} \tag{25}$$

where $\{d_i\}$ and $\{F_i\}$ are $(N_T + N_S)$-order column vectors

$$\{F_i\}_{(N_T+N_S)\times 1} = \{\{f_i\}_{1\times N_T}, \{g_{xi}\}_{1\times N_S}\}^T \tag{26}$$

$$\{d_i\}_{(N_T+N_S)\times 1} = \{\{P(x_i)\}_{1\times N_\Omega}, \{Q(x_i)\}_{1\times N_D}, \{R(x_i)\}_{1\times N_N}, \{0\}_{1\times N_S}\}^T \tag{27}$$

and $[H_{ij}]$ is a $(N_T + N_S) \times (N_T + N_S)$ coefficient matrix

$$[H_{ij}] = \begin{bmatrix} [LN_j(x_i)]_{N_\Omega\times N_T} & \left[L\left(\left(x_i - \sum_{n=1}^{N_T} N_n(x_i)x_n\right)M_j(x_i)\right)\right]_{N_\Omega\times N_S} \\ [N_j(x_i)]_{N_D\times N_T} & [0]_{N_D\times N_S} \\ [0]_{N_N\times N_T} & [M_j(x_i)]_{N_N\times N_S} \\ [N_{j,x}(x_i)]_{N_S\times N_T} & \left[\left(-\sum_{n=1}^{N_T} N_{n,x}(x_i)x_n\right)M_j(x_i)\right]_{N_S\times N_S} \end{bmatrix} \tag{28}$$

By solving numerically the set of linear algebraic eqs. (25), $(N_T + N_S)$ point values $\{F_i\}$ are obtained. Accordingly, the approximate solutions $\tilde{f}(x)$ and the first-order differential $\tilde{g}_x(x)$ can be computed through eqs. (9) and (10), respectively.

Model implementation

To simulate the kinetics of drug release, the nondimensional partial differential governing equation is discretized in spatial domain by the Hermite-cloud method and discretized in time domain by linear interpolation technique. Namely, for the drug release governing eq. (3) at time τ,

$$\frac{\partial\psi(\xi,\tau)}{\partial\tau} = \frac{\partial^2\psi(\xi,\tau)}{\partial\xi^2} + \frac{2}{\xi}\frac{\partial\psi(\xi,\tau)}{\partial\xi} - \beta\psi(\xi,\tau) \tag{29}$$

By using the Hermite-cloud method for spatial discretization, we have

$$\psi(\xi,\tau) = \sum_{n=1}^{N_T} N_n(\xi)\psi_n(\tau) + \sum_{m=1}^{N_S}\left(\xi - \sum_{n=1}^{N_T} N_n(\xi)\xi_n\right) \times M_m(\xi)\psi_{\xi m}(\tau) \tag{30}$$

$$\psi_\xi(\xi,\tau) = \frac{\partial\psi(\xi,\tau)}{\partial\xi} = \sum_{m=1}^{N_S} M_m(\xi)\psi_{\xi m}(\tau) \tag{31}$$

$$\frac{\partial^2\psi(\xi,\tau)}{\partial\xi^2} = \sum_{n=1}^{N_T} N_{n,\xi\xi}(\xi)\psi_n(\tau) \tag{32}$$

TABLE I
Experimental and Identified Parameters of Nifedipine Microgels

Type	Experimental data[6]		Identified parameters		
	R ($\times 10^{-4}$ cm)	M_∞ ($\times 10^{-13}$ g)	D ($\times 10^{-11}$ cm^2/s)	k ($\times 10^{-7}$ s^{-1})	εC_s ($\times 10^{-6}$ g/cm^3)
B1	12.10	0.20	0.40	7.0	1.225
B2	13.90	0.24	0.40	7.0	1.225
B3	13.05	0.20	0.35	7.0	1.033
B4	12.20	0.16	0.30	7.0	0.823
B5	14.50	0.32	0.40	7.0	1.225

Substituting eqs. (30)–(32) into eq. (29), the governing equation is discretized at ξ_i of spatial domain in the following form,

$$\frac{\partial \psi(\xi_i, \tau)}{\partial \tau} = \sum_{n=1}^{N_T} (N_{n,\xi\xi}(\xi_i) - \beta N_n(\xi_i))\psi_n(\tau) + \left(\frac{2}{\xi_i} - \beta\left(\xi_i - \sum_{n=1}^{N_T} N_n(\xi_i)\xi_n\right)\right) \sum_{m=1}^{N_S} M_m(\xi_i)\psi_{\xi m}(\tau) \quad (33)$$

By the linear interpolation technique, a weighted average of the time derivative $\partial\psi/\partial\tau$ can be approximated at two consecutive time steps as follows,[21]

$$(1-\alpha)\frac{\partial \psi(\xi_i, \tau)}{\partial \tau} + \alpha \frac{\partial \psi(\xi_i, \tau + \Delta\tau)}{\partial \tau} = \frac{\psi(\xi_i, \tau + \Delta\tau) - \psi(\xi_i, \tau)}{\Delta\tau} \quad (34)$$

where α is a weighted coefficient ($0 \le \alpha \le 1$).

Substituting eqs. (30) and (33) into eq. (34) and considering the auxiliary condition (18), the governing equation with time iteration is finally discretized in both spatial and time domains and reduced to a set of discrete algebraic equations in the following matrix form,

$$\begin{bmatrix} [G_{ij}^{11}]_{N_T\times N_T} & [G_{ij}^{12}]_{N_T\times N_S} \\ [G_{ij}^{21}]_{N_S\times N_T} & [G_{ij}^{22}]_{N_S\times N_S} \end{bmatrix} \begin{Bmatrix} \{\psi_i(\tau+\Delta\tau)\}_{N_T\times 1} \\ \{\psi_{\xi_i}(\tau+\Delta\tau)\}_{N_S\times 1} \end{Bmatrix} = \begin{bmatrix} [G_{ij}^{*11}]_{N_T\times N_T} & [G_{ij}^{*12}]_{N_T\times N_S} \\ [G_{ij}^{*21}]_{N_S\times N_T} & [G_{ij}^{*22}]_{N_S\times N_S} \end{bmatrix} \begin{Bmatrix} \{\psi_i(\tau)\}_{N_T\times 1} \\ \{\psi_{\xi_i}(\tau)\}_{N_S\times 1} \end{Bmatrix} \quad (35)$$

where

$$[G_{ij}^{11}] = [(1 + \alpha\beta\Delta\tau)N_j(\xi_i) - \alpha\Delta\tau N_{j,\xi\xi}(\xi_i)] \quad (36a)$$

$$[G_{ij}^{12}] = \left[-\frac{2\alpha\Delta\tau}{\xi_i} + (1+\alpha\beta\Delta\tau) \times \left(\xi_i - \sum_{n=1}^{N_T} N_n(\xi_i)\xi_n\right)\right] M_j(\xi_i) \quad (36b)$$

$$[G_{ij}^{21}] = [G_{ij}^{*21}] = [N_{j,\xi}(\xi_i)] \quad (36c)$$

$$[G_{ij}^{22}] = [G_{ij}^{*22}] = \left[\left(-\sum_{n=1}^{N_T} N_{n,\xi}(\xi_i)\xi_n\right) M_j(\xi_i)\right] \quad (36d)$$

$$[G_{ij}^{*11}] = [(1-\alpha)\Delta\tau N_{j,\xi\xi}(\xi_i) + (1 - \beta(1-\alpha)\Delta\tau)N_j(\xi_i)] \quad (36e)$$

$$[G_{ij}^{*12}] = \left[\left(\frac{2(1-\alpha)\Delta\tau}{\xi_i} + (1-\beta(1-\alpha)\Delta\tau) \times \left(\xi_i - \sum_{n=1}^{N_S} N_n(\xi_i)\xi_n\right)\right) M_j(\xi_i)\right] \quad (36f)$$

NUMERICAL SIMULATION

The experimentally measured nifedipine release data for the spherical nifedipine-loaded chitosan microgels exposed to phosphate buffer (pH 7.4), achieved by Filipovic-Grcic et al. through the chitosan microgel preparation and characterization and nifedipine release determination,[6] are simulated numerically by the present mathematical model. A series of B samples (B1–B5) are selected and the corresponding microsphere radii R are listed in Table I.[6] The total loaded drug mass M_∞ listed in Table I is calculated based on the mass of drug-loaded microgels m (g), total drug content d (%), the mean radius of dry microgels R (cm), and the volume of the dissolution medium V (cm^3) obtained from the experimental data.[6] Assuming that all the drug is released and dissolved in the dissolution medium

$$M_\infty = \frac{4}{3} \times \pi \times R^3 \times \frac{m \times d}{V}$$

One is reminded that such an assumption will bring about unpredictable error in M_∞; however, because the ratio of M_t/M_∞ is concerned in this study, this inaccuracy would not affect the prediction.

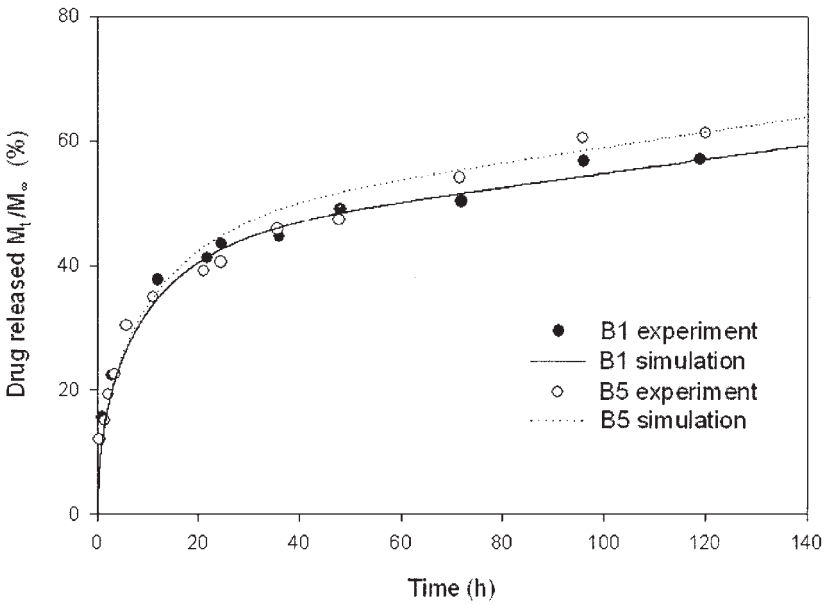

Figure 1 Rate of nifedipine release from chitosan microgels with different radii R.

Identification of physical parameters of model

Figure 1 shows the *in vitro* drug release kinetics from the microgels with different microsphere radii and total initially loaded drug amounts. As the time increases, the initial drug release amount increases rapidly, followed by a gradual drug release. B5 has larger microspheric radius R and higher total loaded drug amount M_∞ (see Table I). It is observed that nifedipine from B5 is released a little faster than that from B1. Good agreement between fitted results and experimental data is obtained for both B1 and B5 with the present mathematical model. It can be seen that the model successfully captures the effect of microspherical radius R. The values of the diffusion coefficient D, drug dissolution rate constant k, and equivalent drug saturation concentration ϵC_s are identified by best-fitting the computed results to the experimental data. The identified D, k, and ϵC_s are summarized in Table I. The D value is found to be smaller than the reported value of nifedipine in crosslinked hydrogels of polyacrylamide-grafted guar gum.[22] Generally, the D values for various drugs in polymeric hydrogels range from 10^{-6} to 10^{-9} cm^2/s. Several factors may contribute to the extremely low D value of nifedipine in the studied microgels. First, the solubility of nifedipine in the release medium is very low (11 μg/mL), which implies relatively a large partition coefficient of nifedipine between the polymeric hydrogels and the release medium. Second, the microgels that are loaded with a high content of drug tend to absorb less water than those containing a lower content of drug; therefore, the diffusion processes are retarded. Last, it is reported that an increase in drug content will also increase the crystallinity of the drug and thus slow down the release of such a crystalline drug.[23]

Figure 2 illustrates the nifedipine release kinetics from chitosan microgels with a different network mesh parameter ϵ. These microgels are formed with the same nifedipine amount but different glutaraldehyde reaction times. With an increase in the glutaraldehyde reaction time, the crosslinking degree of the microgels increases, which brings about a decrease in the network mesh parameter ϵ of the microgels. This results in the decrease of the equivalent saturation concentration ϵC_s. The fitting well represents the experimental results. The corresponding D and ϵC_s are identified by best-fitting the calculating results to the experimental data, and they are summarized in Table I. The diffusion coefficient D is observed to be dependent on the crosslinking density, and thus, on the network mesh parameter ϵ. An increase of ϵC_s from 0.823 to 1.225 increased the D value from 0.30×10^{-11} to 0.40×10^{-11} cm^2/s. An increased network mesh parameter ϵ increases the drug diffusion coefficient D, which is consistent with the findings by Pillay and Fassihi.[24]

Figures 1 and 2 validate that the present mathematical model is able to describe well the nifedipine release from chitosan microgels with different microsphere conditions. It successfully captures the characteristics of the various important physical parameters affecting the nifedipine release kinetics. Therefore, it is concluded that this model provides a suitable simulating approach to obtain deeper insight into the effects of the important physical parameters on drug release from the microgels.

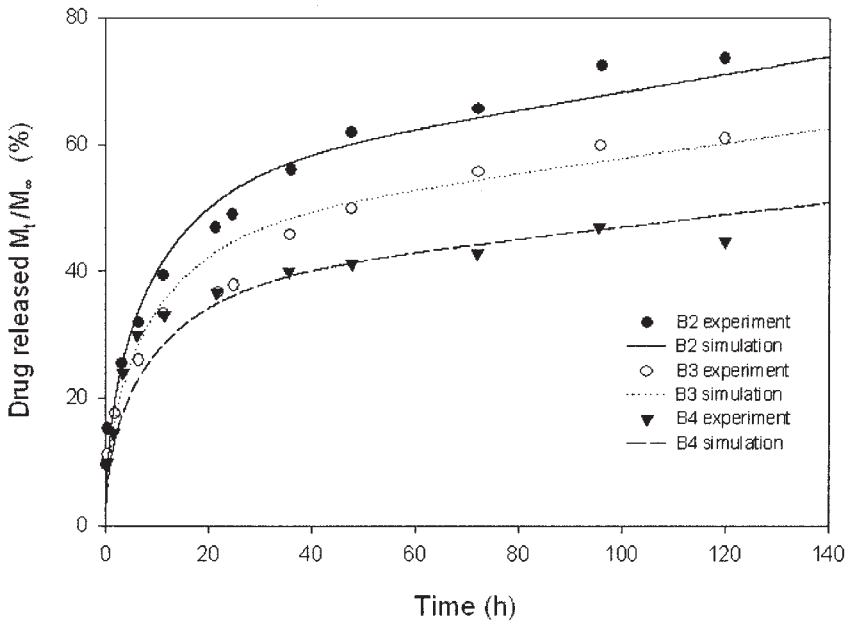

Figure 2 Rate of nifedipine release from chitosan microgels with different network mesh parameter ϵ.

Discussion about effect of physical parameters of model

To study the effect of the physical parameters, including the microsphere radius R, drug diffusion coefficient D, drug dissolution rate constant k, and equivalent saturation concentration ϵC_s, the mathematical model is employed to simulate drug release kinetics. When the sensitivity analysis on one of the parameters is carried out, the other parameters remained the same. In Figures 3-6, the experimental drug release data from the B5 sample are taken as a comparative example.

Figure 3 shows the effect of microspherical radius R on controlled drug release, where the drug diffusion coefficient D is set equal to 0.4×10^{-11} cm^2/s; drug dissolution rate constant k is set equal to 7.0×10^{-7} s^{-1}, and drug equivalent saturation concentration ϵC_s is set equal to 1.225×10^{-6} g/cm^3. The microsphere

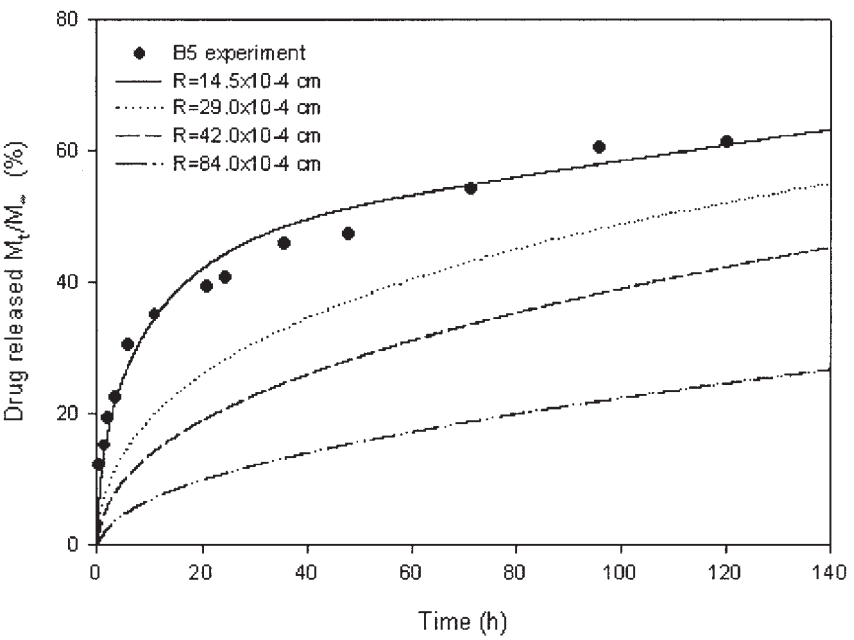

Figure 3 Effect of the microsphere radius R on the rate of nifedipine release from chitosan microgels when $D = 0.4 \times 10^{-11}$ cm^2/s, $k = 7.0 \times 10^{-7}$ s^{-1}, $\epsilon C_s = 1.225 \times 10^{-6}$ g/cm^3.

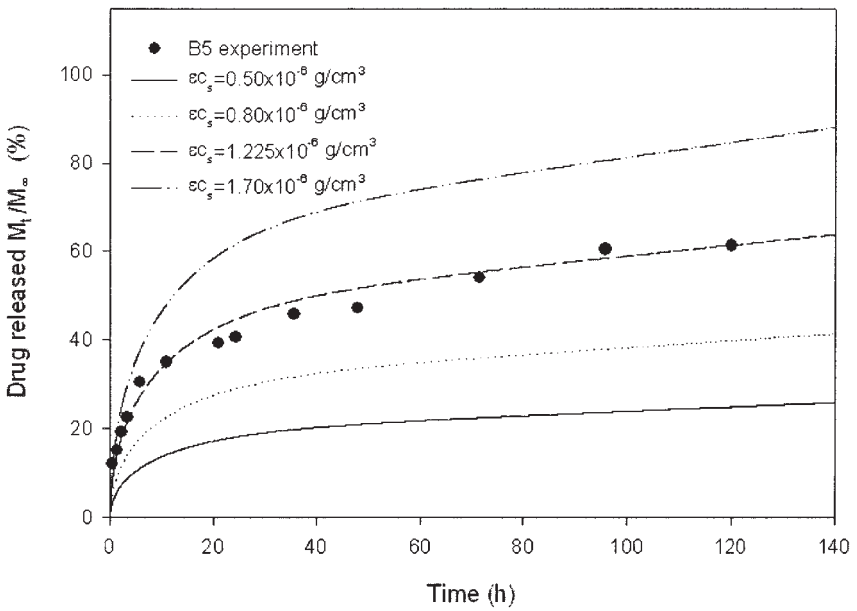

Figure 4 Effect of the equivalent drug saturation concentration ϵC_s on the rate of nifedipine release from chitosan microgels when $D = 0.4 \times 10^{-11}$ cm^2/s, $R = 14.5 \times 10^{-4}$ cm, $k = 7.0 \times 10^{-7}$ s^{-1}.

radius R in the figure ranges from 9.5×10^{-4} to 17.0×10^{-4} cm. By increasing the microsphere radius R, the overall drug release rate becomes slower. It is noted that a slight change of microsphere radius R results in remarkable alteration of nifedipine release rate. A smaller microgel has larger specific surface area of contact with the release medium and would facilitate the drug diffusion through the continuous matrices of microgels into the release medium in comparison with a larger microgel. A decrease in microsphere radius increases both the initial fast release rate and the following gradual release rate. This implies that variation of microspheric radius affects both drug dissolution and diffusion process.

The effect of equivalent drug saturation concentration ϵC_s on drug release kinetics is shown in Figure 4, where the equivalent drug saturation concentration ϵC_s changes from 0.5×10^{-6} to 1.7×10^{-6} g/cm^3. The drug release is remarkably increased with increasing porosity. An increase of the network mesh parameter ϵ of microgels (i.e., a decrease of the crosslinking density of microgels) simultaneously increases the drug equivalent saturation concentration ϵC_s and the drug diffusion coefficient D, which results in an increase in both drug dissolution and diffusion rates. These synergically lead to the increased nifedipine release rate.

Figure 5 is obtained for discussion about the effect of drug diffusion coefficient D on drug release, where the D value varies from 0.012×10^{-11} to 4.0×10^{-11} cm^2/s. It is observed that the diffusion process controls significantly the initial drug release stage. As the diffusion coefficient D increases, the initial drug release rate increases distinctly, and the drug release amount becomes a linear function of time at relatively shorter times. However, after a certain period of release time, the drug release arrives at a constant level. This indicates that the release of drug with low diffusion coefficient D is via diffusion mechanism, whereas the diffusion process does not solely control the release of drug with high diffusion coefficient D.

Figure 6 illustrates the effect of the drug dissolution rate constant k on drug release, where the value of dissolution rate constant k varies from 0.70×10^{-7} to 24.0×10^{-7} s^{-1}. It is manifest that alteration of drug dissolution rate constant k has insignificant effects on initial drug release rate. However, after a period of release time, the drug release rate increases with increasing dissolution rate constant k. This indicates that different mechanisms control different drug release stages. At the initial stage, diffusion through continuous matrices of microgels predominantly affects the drug release, but after a period of drug release, drug dissolution starts to significantly affect the drug release rate.

CONCLUSION

The present mathematical model based on drug dissolution and diffusion through the continuous matrices of microgels is well validated by comparison with the experimental nifedipine release from the spherical nonswellable chitosan microgels. It provides a better understanding of the underlying mechanisms in microspheric drug release system and represents a high-efficiency tool to study the roles played by important characteristics of the drug and the microgels such as

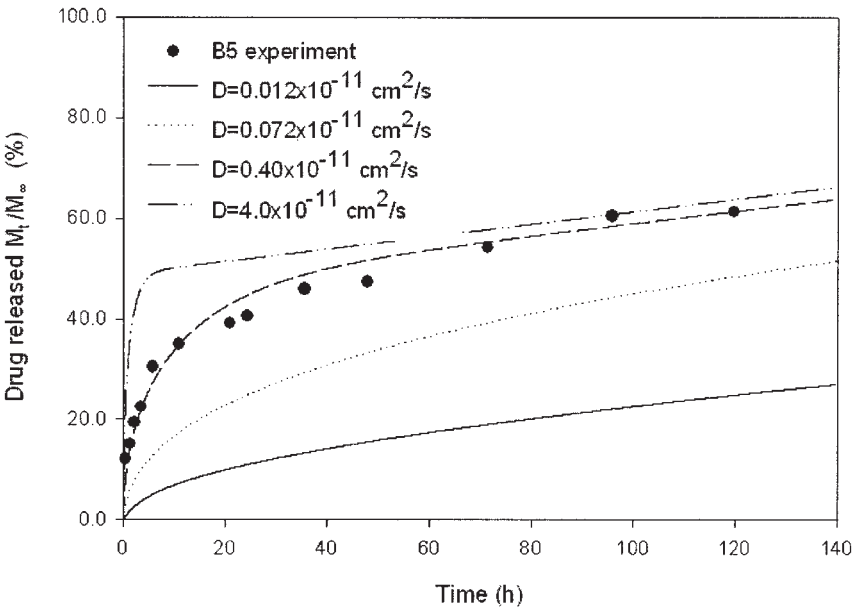

Figure 5 Effect of the diffusion coefficient D on the rate of nifedipine release from chitosan microgels when $R = 14.5 \times 10^{-4}$ cm, $k = 7.0 \times 10^{-7}$ s^{-1}, $\epsilon C_s = 1.225 \times 10^{-6}$ g/cm^3.

the diffusion coefficient, the microspherical radius, and the network mesh parameter. Consequently, it can be used to analyze and optimize the design of the controlled drug release process.

NOTATION

A area of microgels, cm^2
C concentration of solute dissolved in microgels, g/cm^3
C_0 initial solute loading in microgels, g/cm^3
C_s drug saturation concentration in microgels, g/cm^3
D drug diffusion coefficient, cm^2/s
J drug diffuse flux, g/cm^2/s
k dissolution rate constant, s^{-1}
M_t absolute cumulative amount of drug released at time t, g
M_∞ absolute cumulative amount of drug released at time $t = \infty$, g

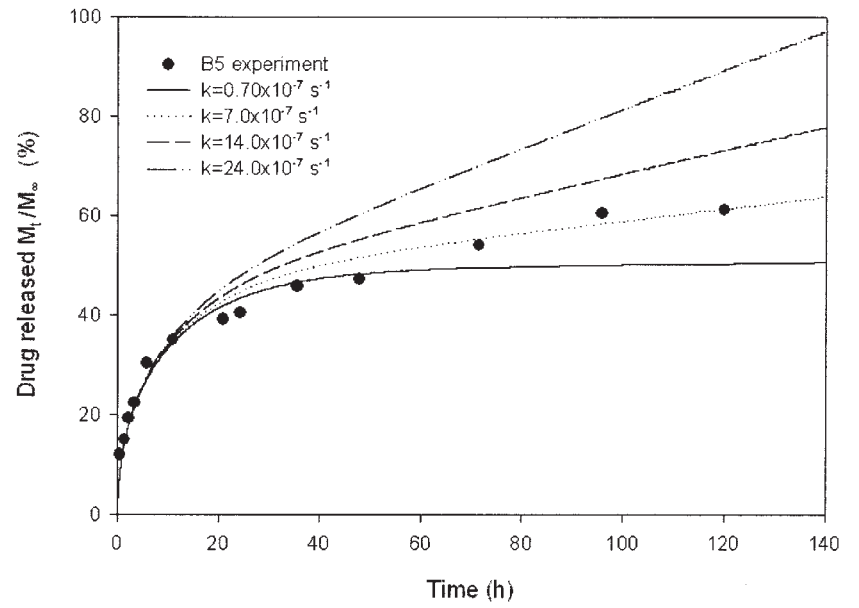

Figure 6 Effect of the dissolution rate constant k on the rate of nifedipine release from chitosan microgels for $R = 14.5 \times 10^{-4}$ cm, $D = 0.4 \times 10^{-11}$ cm^2/s, $\epsilon C_s = 1.225 \times 10^{-6}$ g/cm^3.

r radial position in spherical microgels, cm
t release time, s
α a weighted coefficient ($0 \leq \alpha \leq 1$)
β dimensionless dissolution/diffusion number
ϵ network mesh parameter of microgels
ϵC_s equivalent drug saturation concentration, g/cm^3
ξ dimensionless radius
τ dimensionless Fourier time
ψ dimensionless concentration
m mass of drug-loaded microgels, g
d total drug content, %
V volume of the dissolution medium, cm^3
R mean radius of dry microgels, cm

References

1. Liu, L. X.; Ku, J.; Khang, G.; Lee, B.; Rhee, J. M.; Lee, H. B. J Controlled Release 2000, 68, 145.
2. Hombreiro-Perez, M.; Siepmann, J.; Zinutti, C.; Lamprecht, A.; Ubrich, N.; Hoffman, M.; Bodmeier, R.; Maincent, P. J Controlled Release 2003, 88, 413.
3. Mansoor, A. F.; von Hagel Keefer, L. A. Pharmacol Ther 2002, 27, 362.
4. Grossman, E.; Messerli, F. H.; Grodzicki, T.; Kowey, P. JAMA 1996, 276, 1328.
5. Okada, H.; Yamamoto, M.; Heya, T.; Inoue, Y.; Kamei, S.; Ogawa, Y.; Toguchi, H. J Controlled Release 1994, 28, 121.
6. Filipovic-Grcic, J.; Becirevic-Lacan, M.; Skalko, N.; Jalsenjak, I. Int J Pharm 1996, 135, 183.
7. Chandy, T.; Sharma, C. P. Biometerials 1992, 13, 949.
8. Chowdary, K. P. R.; Sankar, G. G. Drug Dev Ind Pharm 1997, 23, 325.
9. Dhawan, S.; Singla, A. K. Biotechnic & Histochem 2003, 78, 243.
10. Soppimath, K. S.; Aminabhavi, T. M. J Microencapsul 2002, 19, 281.
11. Varshosaz, J.; Falamarzian, M. Eur J Pharmaceutics and Biopharmaceutics 2001, 51, 235.
12. Harland, R. S.; Dubernet, C.; Benoit, J. P.; Peppas, N. A. J Controlled Release 1988, 7, 207.
13. Higuchi, T. J Pharm Sci 1961, 50, 874.
14. Roseman, T. J.; Higuchi, W. I. J Pharm Sci 1970, 59, 353.
15. Higuchi, W. I. J Pharm Sci 1962, 51, 802.
16. Grassi, M.; Colombo, I.; Lapasin, R. J Controlled Release 2000, 68, 97.
17. Crank, J. The Mathematics of Diffusion, 2nd ed.; Clarendon Press: Oxford, 1975.
18. Robert, A. A. Physical Chemistry, 2nd ed.; Wiley: New York, 1996.
19. Li, H.; Ng, T. Y.; Cheng, J. Q.; Lam, K. Y. Comput Mech 2003, 33, 30.
20. Ng, T. Y.; Li, H.; Cheng, J. Q.; Lam, K. Y. Eng Struct 2003, 25, 141.
21. Reddy, J. N. An Introduction to the Finite Element Method, 2nd ed.; McGraw-Hill: New York, 1993.
22. Soppimath, K. S.; Kulkarni, A. R.; Aminabhavi, T. M. J Controlled Release 2001, 75, 331.
23. Soppimath, K. S.; Kulkarni, R. A.; Sminsbhavi, T. M. J Biomat Sci Polym Ed 2000, 11, 27.
24. Pillay, V.; Fassihi, R. Pharm Res 1999, 16, 333.